



ESTIMATION OF THE TSUNAMI SOURCE OF THE 1979 GREAT TUMACO EARTHQUAKE USING TSUNAMI NUMERICAL MODELING

B. Adriano⁽¹⁾, M. Arcila⁽²⁾, R. Sanchez⁽³⁾, E. Mas⁽⁴⁾, S. Koshimura⁽⁵⁾, P. Arreaga⁽⁶⁾, and N. Pulido⁽⁷⁾

⁽¹⁾ Postdoc Researcher, International Research Institute of Disaster Science, Tohoku University, e-mail: adriano@irides.tohoku.ac.jp

⁽²⁾ Geóloga, Servicio Geológico Colombiano, Colombia, e-mail: marcila@sgc.gov.co

⁽³⁾ Investigador, Dirección General Marítima (DIMAR), Colombia, e-mail: rsanchez@dimar.mil.co

⁽⁴⁾ Assistant Professor, International Research Institute of Disaster Science, Tohoku University, e-mail: mas@irides.tohoku.ac.jp

⁽⁵⁾ Professor, International Research Institute of Disaster Science, Tohoku University, e-mail: koshimura@irides.tohoku.ac.jp

⁽⁶⁾ Oceanógrafa, Instituto Oceanográfico de la Armada (INOCAR), Ecuador, e-mail: patricia.arreaga@gmail.com

⁽⁷⁾ Research Seismologist, National Research Institute for Earth Science and Disaster Prevention (NIED), e-mail: nelson@bosai.go.jp

Abstract

The 1979 Great Tumaco earthquake occurred on 12 December recorded as a surface-wave magnitude of $M_s 7.7$, and moment magnitude $M_w 8.1$ reported in the Harvard CMT Catalog. The epicenter was located 80 km southwest of Tumaco, offshore the Pacific coast of Colombia. This event generated a tsunami that killed more than 220 residents of San Juan island, 60 km north of Tumaco. According to eyewitnesses, few minutes after the event the sea withdrew from the shoreline, then, it returned 10 to 15 minutes later in a succession of three to four cycles of waves. The observed maximum inundation height at this area was approximately 2.5 m. In addition, due to the coseismic crustal subsidence of approximately 1.2 to 1.6 m, streets and houses were inundated over a meter of water depth. Within the framework of the project “Application of State of the Art Technologies to Strengthen Research and Response to Seismic, Volcanic and Tsunami Events, and Enhance Risk Management in Colombia” (JST-JICA SATREPS), the tsunami source model of the 1979 great Tumaco earthquake was estimated from tsunami waveform records and coseismic crustal deformation data. First, a rupture fault of 250 km by 100 km was assumed, and then, to estimate the slip distribution, we divided the tsunami source into 5 subfaults of 50 km by 100 km size. The focal mechanisms of these subfaults are taken from the Harvard CMT solution (strike=30, dip angle=16, and rake=118). We conducted linear tsunami waveform inversion to reproduce the tsunami source using the recorded tsunami wave at Esmeraldas tide gauge station in Ecuador, which is located approximately 75 km south from the epicenter, and three coastal subsidence point in Colombia. The inversion result showed a maximum slip of 2.9 m in the central area of the fault. The estimated seismic moment was calculated as 2.20×10^{21} Nm ($M_w=8.16$). In addition, the maximum tsunami height estimated from the slip distribution reached up to 8.0 m near San Juan island.

Keywords: The 1979 Great Tumaco earthquake, Tsunami numerical modeling, Tsunami waveform inversion



1. Introduction

The Ecuador-Colombia subduction zone has mainly experimented 4 significant earthquakes during the last 20th century (Fig.1). Starting from the 1906 earthquake with (Mw8.8) with approximately 400 km of rupture area, the 1948 (Mw7.8), the 1958 (Mw7.6), and the 1979 Great Tumaco earthquake (Mw8.2) (Chlieh et al., [1]). The latest occurred off the south coast of Colombia on December 12, 1979 at 07:59:03 UTC (2:59:03 local time) with epicenter 1.68° S 79.36° W according to the Colombian Geological Service (SGC) catalog. This earthquake generated a tsunami that left more that 300 persons dead in southern coast of Colombia (Pararas-Carayamis, [2], Herd et al., [3], INGEOMINAS, [4]). The San Juan island was one of the most affected areas by the earthquake and subsequently tsunami, it was reported that tsunami waves completely overrun the island coursing a completely devastation within the flooded area (Pararas-Carayamis, [2]). According to eyewitnesses testimonies, the first wave of approximately 5 m high arrived at this location about 10 minutes after the mainshock. The tsunami also caused severe damage to Tumaco island, about 50 km to the northeast of the epicenter, where 36 deaths were due to the tsunami (Ramirez and Goberna, [5]). Moreover, the tide gauge station in Tumaco was destroyed by ground shaking as a result, in case of the near-field tsunami, the tsunami wave was only recorded at Esmeraldas tide gauge station in Ecuador, about 75 km to the southwest of the epicenter (Fig.1). The crustal deformation associated to the 1979 earthquake was measured at several location along Colombia coast, mainly to the north of the epicenter. According with several reports, approximately 1.5 m and 0.8 m of land subsidence were observed around San Juan and Tumaco islands, respectively.

The purpose of this study is estimate the slip distribution for the tsunami source due to the 1979 Great Tumaco earthquake. We conduct a joint inversion of tsunami waveform and coastal subsidence values. The inversion analysis is based on the linear approximation of the shallow-water theory. Finally, the maximum tsunami heights are calculated using the tsunami source result, and compared with reported tsunami height at several locations.

2. Data

2.1 Tide Gauge and Ground Deformation Data

The tsunami generated by the 1979 Great Tumaco earthquake was recorded at Esmeraldas tide gauge station in Ecuador. Note that this station is located to the south of the epicenter (Fig.2). We pre-processed this record to retrieve the tsunami signal as follows. We first digitized the tsunami waveform from Pararas-Carayamis, [2]. Then we approximate the tidal record as a polynomial function, and remove it from the original record. Finally, we removed the origin time of the earthquake (Fig.4a). It is important to mention that due to the low quality of the tsunami waveform graph, some information contained in intervals less than 10-minutes was lost. Nevertheless, considering that incoming tsunami waves at coastal areas have characteristic periods of 40-50 minutes (Adriano et al., [6]), the digitized waveform was resampled to 1-minute interval.

We used coastal subsidence data at 3 location collected by the Institute of Geology and Mining of Colombia (INGEOMINAS) [4]. These subsidence points are in different locations along Colombia coast. Note that all the points are located to the northeast of the epicenter (Fig.1). Their geographical coordinates however are based on testimonies of local residents. According with INGEOMINAS's report, the largest subsidence of 1.5 m was located at San Juan island, and subsidence values of 0.8 m and 0.5 m was observed around Tumaco and El Charco islands, respectively.

3. Method

3.1 Fault Parameters

We first estimate the extent of the tsunami source area based on the earthquake moment magnitude and the scaling relation proposed by Murotani et al., [7]. The estimated tsunami source for an earthquake of Mw8.2 is approximately 247 km x 100 km. In this study, considering the aftershocks distribution, we assumed a source area

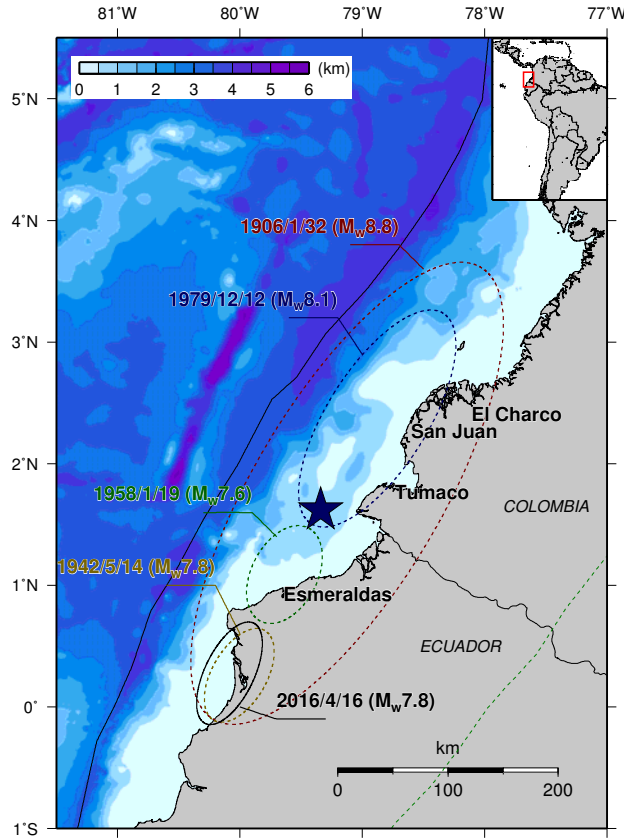


Fig. 1 – Computational region for tsunami waveform inversion. The dashed ellipses show the historical earthquakes along the Nazca subduction zone in Ecuador-Colombia. The blue star shows the epicenter of the 1979 Great Tumaco earthquake. The 2016 Ecuador earthquake is shown in solid black ellipse.

of 250km x 100 km. To estimate slip distribution, we divide the source region into 5 subfaults along the strike (Fig.2). The top depth of the subfaults is 1 km. The strike of 30°, dip angle of 16°, and rake angle of 118° area taken from the Global CMT moment tensor solution and are constant for each subfault (Table 1).

3.2 Tsunami Numerical Simulation

To calculate the tsunami propagation from the source area, a set of linear shallow-water long-wave equations are numerically solved by a finite-difference method using a spherical coordinate system (Satake, [8], Fujii and Satake, [9]). The equation of motion and equation of continuity are expressed by Eq. (1) and Eq. (2), respectively.

$$\frac{\partial V}{\partial t} = -g \nabla h \quad (1)$$

$$\frac{\partial h}{\partial t} = -d \nabla \cdot V \quad (2)$$

Where V is the depth-average horizontal vector velocity, h is the water elevation or tsunami amplitude, d is the water depth, and g is the gravitational acceleration. The computational area extents from 1° S to 5.5° N and 81.5° W to 77° W (Fig.1). The bathymetry grid is 12 arc-second (approximately 370 m); hence, there are 1350 x 1900 grid points along the longitude and latitude directions, respectively. Static deformation of seafloor from each

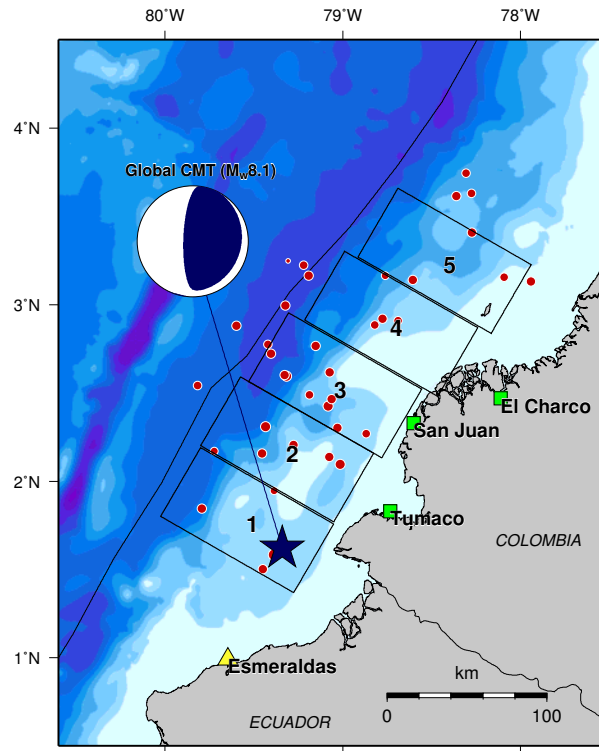


Fig. 2 – Configurations of subfault models used in this study are shown by black rectangles. The location of Esmeraldas tide gauge station is shown by the yellow triangle. The green rectangles show the location of the subsidence points used in this study. The blue star shows the epicenter of the 1979 Great Tumaco Earthquake. The red circles indicate aftershocks within approximately one month after the mainshock (Herd et al., [3]). Black line indicates plate boundary of Nazca and South America Plates.

subfault was calculated using a rectangular fault model (Okada, [6]). This provides the initial condition for the tsunami numerical computation, assuming that the initial water height distribution is the same as that of the seafloor. In addition, we also include the effects of coseismic horizontal displacement in regions of steep bathymetric slopes according to Tanioka and Satake, [7]. In the tsunami propagation modeling, the computation time step was set as 2 s to satisfy the stability condition for the finite-difference method.

3.2 Tsunami Waveform Inversion Method

We used non-negative least square method (Lawson and Hanson, [10]) and delete-half jackknife method (Tichelaar, and Ruff, [11]) to estimate the slip and error, respectively; the details of inversion method are described in Fujii and Satake [12] and Adriano et al., [13]. The observed tsunami waveforms at tide gauges were sampled at 1 min interval, hence the synthetic waveforms are also computed at 1 min interval. Due to the coarse spatial resolution of the bathymetry data (~370 m) around coastal tide gauge station may prevent accurate modeling of later phases such as reflected waves, we used the first cycle of tsunami waveform. Finally, in the joint inversion of tsunami waveform and coseismic crustal deformation (land subsidence), the total number of data points used for the inversion is 53. To perform the tsunami numerical simulation, the 30 arc-second of spatial resolution bathymetry data was taken from the General Bathymetric Chart of the Oceans (GEBCO) [14]. Considering that the phase velocity of the shallow-water wave depends only on the water depth, we prepared a 12 arc-second of spatial resolution by resampling the original GEBCO data (Fig.1).

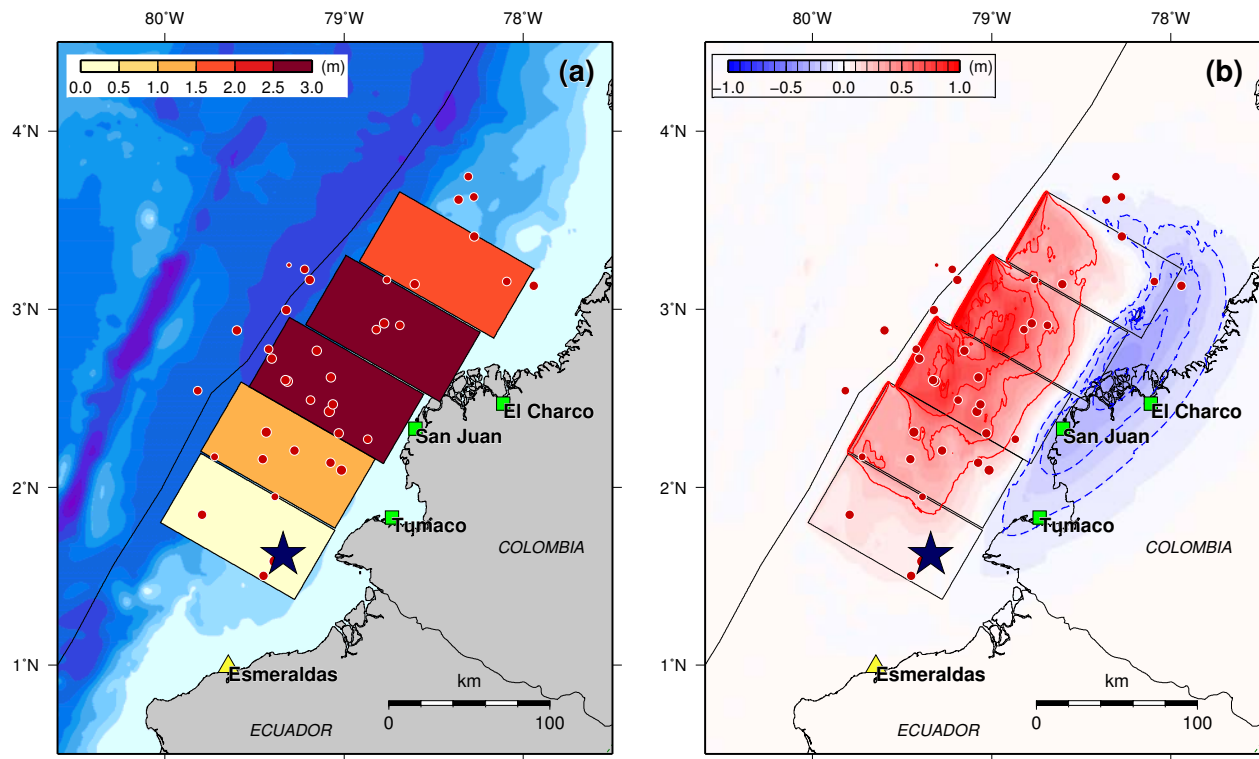


Fig. 3 –(a) Slip distribution estimated by joint inversion of the tsunami waveform at Esmeraldas tide gauge station and coastal land subsidence at three locations (Tumaco, San Juan, and El Charco towns). (b) Crustal deformation computed from the estimated slip distribution. The red solid contours indicate uplift with a contour interval of 0.2 m, whereas the blue dashed contours indicate subsidence, with a contour interval of 0.1 m. The red circles indicate the aftershocks distribution within approximately one month. (Herd et al., [3]).

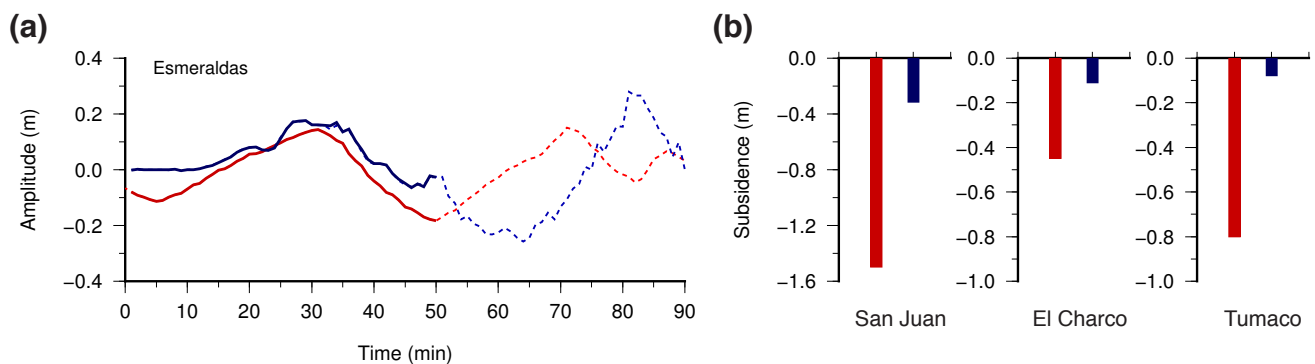


Fig. 4 – (a) Comparison of the observed (red curve) and synthetic (blue curve) tsunami waveform computed from the estimated slip distribution. Time ranges shown by solid curves are used for the inversions (50 minutes); the dashed parts are not used for the inversions, but shown for comparison. (b) Comparison of the reported (red bars) and estimated (blue curve) coseismic land deformation at three different locations. One point from each location was used in the inversion.

Table 1 – Subfault location, focal paramter angles, depth, slip, and error for the tsunami genrerated by the 1979 Great Tumaco Tsunami earthquake.

No.	Lat.* (° N)	Lon.* (° W)	Strike (°)	Dip (°)	Rake (°)	Depth (km)	Slip (m)	Error (+/-)
1	1.80	80.02	30.0	18.0	118.0	1.0	0.37	0.16
2	2.20	79.80	30.0	18.0	118.0	1.0	1.31	0.45
3	2.56	79.52	30.0	18.0	118.0	1.0	2.55	0.88
4	2.91	79.21	30.0	18.0	118.0	1.0	2.90	1.23
5	3.27	78.91	30.0	18.0	118.0	1.0	1.68	0.78

*Location [latitude (Lat.) and longitude (Lon.)] indicates the southwest corner of each subfault

4. Results and Discussion

4.1 Inversion Results

Inversion of tsunami waveforms shows two large slip regions; the first one is in the central part of the source area in front of San Juan island, and the second one is to the north, near the coastal area of the El Charco town. (Fig.3a; Table 1). The large slip area between San Juan and El Charco suggests that the rupture process occurred from south to northeast, which was also indicated by Beck and Ruff, [15]. Assuming an instantaneous rupture model, the largest slip of 2.9 m is estimated on the 4th subfault. The total seismic moment is calculated from this slip distribution as 2.20×10^{21} Nm ($M_w=8.16$), assuming the rigidity of 5.0×10^{10} N/m², which is similar to the one proposed in the Global CMT catalog (1.69×10^{21} Nm).

The comparison between the synthetic and observed data is shown in Fig. 4. The synthetic tsunami waveform at Esmeraldas station generally agree with the recorded one (Fig4a). Although, the initial negative signal is not well reproduced, the amplitude and phase of the first cycle are well explained. It is important to mention that the waveform at this station was resampled from 10-minutes to 1-minute interval, which may explain the low reproducibility of the recorded tsunami signal within the first 10 minutes. On the other hand, the reported land subsidence values are underestimated by the inversion results, the estimated subsidence values are 31 cm, 11 cm, and 8 cm for San Juan, El Charco and Tumaco locations, respectively (Fig.4b). To analysis the ground deformation field around the coastal area, we calculate the crustal deformation computed from the estimated slip distribution (Fig.3b). It shows that the maximum subsidence of 60 cm around San Juan island area, which also underestimates the maximum reported land subsidence in INGEOMINAS, [4]; and Herd et al., [3]. This fact may indicate that a single fault geometry along the strike direction does not properly solve the observed ground deformation.

4.1 Tsunami Characteristics

Figure 5 shows maximum tsunami height calculated from the slip distribution. The tsunami peaks reported from eyewitnesses are well reproduced at the coastal areas of Tumaco and San Juan (Fig. 5b). Our modeling suggested that the maximum tsunami height at Tumaco island is approximately 3.3 m. Furthermore, at San Juan island the tsunami wave height reached up to approximately 6.0 m, which would be high enough to complete overrun this island as described by Pararas-Carayamis, [2], the reported tsunami height in this area was 5 m. The maximum estimated tsunami heights along Colombia coast are between Tumaco and El Charco, reaching values up to 8.0 m at areas near San Juan island. On the order hand, in Ecuador coastal area (south of the tsunami source area), the maximum tsunami height reach up to 2.0 m.

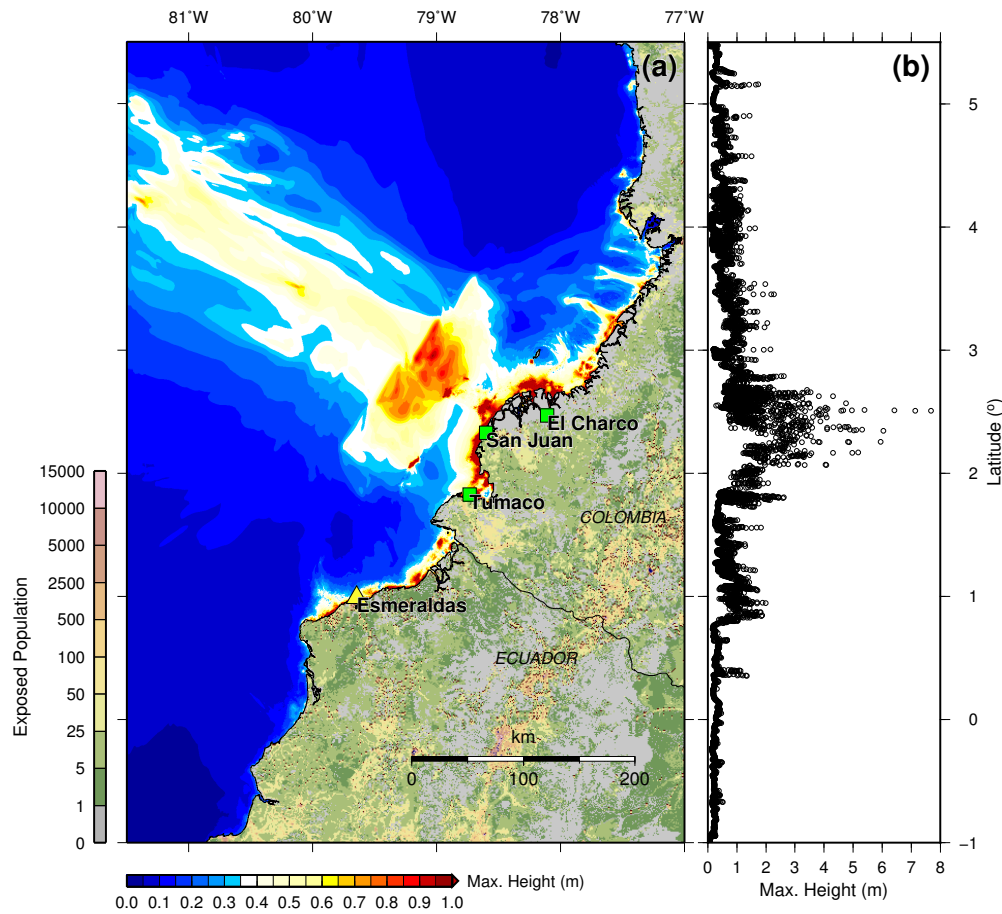


Fig. 5 – (a) Maximum tsunami height calculated from the estimated slip distribution. The exposed population was taken from the global population distribution data (LandScan dataset 2011). (b) Maximum tsunami height at coastal points along the Ecuador and Colombia coastline.

5. Final Comments

We have estimated the tsunami source of the 1979 Great Tumaco Earthquake by using a joint inversion of a single tsunami waveform at Esmeraldas tide gauge station and crustal deformation at three different locations. Inversion result indicates that the 1979 tsunami source was about 250 km long, extending from the epicenter to northeast. For instantaneous rupture model, the largest slip was estimated as 2.9 m in the central area of the fault, up to 0.4 m around the epicenter. The tsunami simulation from the slip distribution showed maximum tsunami height of 8.0 m around El Charco coastal area. Furthermore, the estimated tsunami height at Tumaco and San Juan areas were consistent with reported ones.

6. Acknowledgements

This research was supported by the Japan Society for the Promotion of Science (JSPS) under the project: Fusion of Real-time Simulation and Remote Sensing for Tsunami Damage Estimation to Latin America (JSPS-grant: P16055). Additionally, most of the data used in this study was provided within the framework of the SATREPS project, Application of State of the Art Technologies to Strengthen Research and Response to Seismic, Volcanic and Tsunami Events, and Enhance Risk Management in Colombia, sponsored by the Japan International Cooperation Agency and the Japan Science and Technology Agency.



7. References

- [1] Chlieh M., Mothes P. A., Nocquet J. M., Jarrin P., Charvis P., Cisneros D., Font Y., Collot J. Y., Villegas-Lanza J. C., Rolandone F., Vallée M., Regnier M., Segovia M., Martin X., and Yepes H. (2014): Distribution of discrete seismic asperities and aseismic slip along the Ecuadorian megathrust. *Earth Planet. Sci. Lett.*, vol. 400, pp. 292–301.
- [2] Pararas-Carayannis G. (1980): Earthquake and Tsunami of 12 December 1979 in Colombia. *International Tsunami Information Center*.
- [3] Herd D. G., Youd T. L., Meyer H., Person J. L. C, W. J., and Mendoza C. (1981): The great tumaco, Colombia earthquake of 12 december 1979. *Science*, vol. 211, no. 4481, pp. 441–445.
- [4] Instituto Colombiano de Geología y Minería (INGEOMINAS) (2007)" Estudio Macrosísmico del Sismo del 12 de Diciembre de 1979 en el Océano Pacífico.
- [5] Ramirez J. E. and Goberna J. R. (1980): Terremotos Colombianos Noviembre 23 y Diciembre 12 de 1979; Informe Preliminar. *Instituto Geofísico de los Andes Colombianos, Universidad Javeriana*.
- [6] Adriano B., Mas E., Koshimura S., Fujii Y., Yauri S., Jimenez C., and Yanagisawa H. (2013) Tsunami inundation mapping in Lima, for two tsunami source scenarios. *J. Disaster Res.*, vol. 8, no. 2, pp. 274–284.
- [7] Murotani S., Satake K., and Fujii Y. (2013): Scaling relations of seismic moment, rupture area, average slip, and asperity size for $M \sim 9$ subduction-zone earthquakes. *Geophys. Res. Lett.*, vol. 40, no. 19, pp. 5070–5074.
- [8] Satake K. (1995): Linear and nonlinear computations of the 1992 Nicaragua earthquake tsunami. *Pure Appl. Geophys. PAGEOPH*, vol. 144, no. 3–4, pp. 455–470.
- [9] Fujii Y. and Satake K. (2007): Tsunami Source of the 2004 Sumatra-Andaman Earthquake Inferred from Tide Gauge and Satellite Data. *Bull. Seismol. Soc. Am.*, vol. 97, no. 1A, pp. S192–S207.
- [10] Lawson C. L. and Hanson R. J. (1995): Solving Least Squares Problems. *Society for Industrial and Applied Mathematics*.
- [11] Tichelaar B. W. and Ruff L. J. (1989): How good are our best models? Jackknifing, bootstrapping, and earthquake depth. *Eos, Trans. Am. Geophys. Union*, vol. 70, no. 20, p. 593.
- [12] Fujii Y. and Satake K. (2006): Source of the July 2006 West Java tsunami estimated from tide gauge records. *Geophys. Res. Lett.*, vol. 33, no. 24, pp. 1–5.
- [13] Adriano B., Mas E., Koshimura S., Fujii Y., Yanagisawa H., and Estrada M. (2016): Revisiting the 2001 Peruvian Earthquake and Tsunami Impact Along Camana Beach and the Coastline Using Numerical Modeling and Satellite Imaging. *Tsunamis and Earthquakes in Coastal Environments*, pp. 1–16.
- [14] British Oceanographic Data Centre (1997): The Century Edition of the GEBCO Digital Atlas.
- [15] Beck S. L. and Ruff L. J. (1984): The rupture process of the Great 1979 Colombia Earthquake: Evidence for the asperity model. *J. Geophys. Res.*, vol. 89, no. B11, p. 9281.